Nuclear levels of ^{239}Np excited by the (^{3}He, d) and (α, t) reactions*

T. von Egidy
Physik-Department, Technische Universität München, Germany

Th. W. Elze
Institut für Kernphysik, Universität Frankfurt, Germany

J. R. Huizenga
Nuclear Structure Research Laboratory† and Departments of Chemistry and Physics, University of Rochester, Rochester, New York 14627

(Received 31 October 1974)

The single proton transfer reactions ^{238}U(^{3}He, d)^{239}Np and ^{238}U(α, t)^{239}Np have been measured with 28.5-MeV ^{3}He and α particles, respectively. The experimental cross sections are compared with theoretical cross sections in order to determine l values and to construct a level scheme of ^{239}Np. The configurations $5/2^+[642\uparrow]$, $5/2^-[523\downarrow]$, $1/2^-[530]$, and $3/2^-[521\uparrow]$ are identified. Levels of the four additional rotational bands $1/2^+[400]$, $3/2^+[651\uparrow]$, $7/2^+[633\uparrow]$, and $7/2^-[514\downarrow]$ are assigned tentatively. A level scheme of ^{239}Np containing γ rays following the β decay of ^{239}U is presented also.

[NUCLEAR REACTIONS ^{238}U(^{3}He, d), ^{238}U(α, t), E = 28.5 MeV; measured $\sigma(\theta)$, deduced l values, Nilsson configurations, and level scheme of ^{239}Np.]

I. INTRODUCTION

Models for deformed nuclei, in particular the Nilsson model, can be tested by studying the single-particle structure of the actinides.[1] This is important for the extrapolation of these models to superheavy nuclei. Recent publications[2,3] have shown that the structure of odd-proton actinides can be elucidated by studying the (^{3}He, d) and (α, t) reactions. The combination of such experiments with results from α and β decay allows one to identify rotational bands and to determine spectroscopic factors.

The level scheme of ^{239}Np has been studied previously by β decay[4-8] and α decay.[9-16] These measurements led to the identification of two rotational bands; namely, the ground state $\frac{5}{2}^+[642\uparrow]$ band and the $\frac{5}{2}^-[523\downarrow]$ band. The latter band is the favored band in α decay from ^{243}Am. The level scheme of ^{239}Np is very similar to that of ^{237}Np where more rotational bands are confirmed.[17]

In the present paper we report measurements on the ^{238}U(^{3}He, d)^{239}Np and ^{238}U(α, t)^{239}Np reactions in order to complement the level scheme data from the radioactivity measurements.

II. EXPERIMENT

The experiments were performed with the University of Rochester Emperor tandem accelerator. The experimental technique has been described previously.[2,3] A natural uranium target (thickness $\approx$50 μg/cm^2 on 20-μg/cm^2 carbon backing) was bombarded with 28.5-MeV ^{3}He and α particles for the (^{3}He, d) and (α, t) reactions, respectively. The deuterons and tritons were recorded on photographic plates with an Enge split-pole spectrograph and the plates were scanned with a microscope. The (^{3}He, d) and (α, t) spectra measured at 60° are shown in Fig. 1. These spectra were evaluated by computer with fit programs. The (^{3}He, d) reaction was measured at laboratory angles of 20°, 35°, 60° (three separate experiments), and 90°, and the (α, t) reaction at a laboratory angle of 60°. Elastically scattered ^{3}He and α particles, respectively, were counted simultaneously to obtain absolute cross sections. Lines from light element impurities in the target are easily identified because of their broader linewidth.

Energies and differential cross sections of the observed lines below 1200-keV excitation energy are listed in Table I. The ratio $R = d\sigma(\alpha, t)/d\sigma(^3\text{He}, d)$ (60°) is also given in this table. From a comparison of this ratio R and of the angular distribution with distorted-wave Born-approximation (DWBA) calculations a probable l value was deduced. The DWBA cross sections will be discussed in Sec. III. A detailed angular distribution was not measured because, in the present case, this does not yield much additional information on the l value over that obtained from the four (^{3}He, d) angles and the R ratios.

The experimental energies in Table I were obtained by the following procedure: The positions in the photographic plate were converted into excitation energies by a relativistic kinematic calcu-

lation using the reaction Q values[18] and the dispersion function of the spectrograph. These excitation energies were slightly shifted in such a way that the strong 521.2-keV line had the same position in all spectra. Then, the energies were averaged [weighted with $1/(\Delta E)^2$]. The averaged energies were adjusted with a linear function so that 10 lines (27.9; 70.0; 117.8; 173.7; 449.8; 695.4; 823.4; 992.9; and 1049.0 keV) corresponded best to the energies obtained in the γ-decay scheme (see Fig. 3 and Sec. IV). It is not known if all 10 levels correspond to the levels in the decay scheme, but there is a large probability that at least the majority of lines are correctly assigned. The energy errors include the statistical error and the error of the calibration.

III. THEORETICAL CALCULATIONS OF THE CROSS SECTIONS AND SINGLE-PARTICLE ENERGIES

The theoretical differential cross sections of the (^{3}He, d) and (α, t) reactions are calculated with the following formula[2,19]:

$$(d\sigma/d\omega)_{0^+\to J} = 2C_{jl}{}^2 U^2 N \sigma_{\mathrm{DWBA}}(l, \theta, Q).$$

In the case of Coriolis mixing the factor $S_{jl} = 2C_{jl}{}^2U^2$ has to be replaced by $S_{jl}^C = 2(\sum_i a_i C_{jl,i} U_i)^2$ (see Ref. 19). The quantity $S_{jl}/(2j+1)$ corresponds to the spectroscopic factor. Nonlocality effects of the present reactions are negligible and not included in the DWBA cross sections. The finite range effects are essentially constant for all l values in each reaction and to a good approximation independent of the angle. Therefore, these effects are incorporated into the normalization constant N of each reaction.

A. σ_{DWBA}

The DWBA cross section σ_{DWBA} depends on the Q value, the l value, the angle θ, and on the type of the reaction. All values of the DWBA cross section were calculated with the computer code DWUCK and optical parameters from the literature.[20,21] Cross sections were computed for excitation energies of 0 keV and 1000 keV, and for other energies the cross sections were obtained by a linear interpolation.

B. C_{jl}

The C_{jl} values were calculated with a computer program by Nilsson[22] with the parameters[23]

$$\epsilon_2 = 0.225, \quad \epsilon_4 = -0.040, \quad \kappa = 0.0577, \quad \mu = 0.650.$$

C. U^2

The pairing emptiness U^2 was estimated from single-particle energies according to the simple pairing formula[19]:

$$U_i{}^2 = \frac{1}{2}\left\{1 + \frac{\epsilon_i - \lambda}{[(\epsilon_i - \lambda)^2 + \Delta^2]^{1/2}}\right\}. \tag{1}$$

The pairing gap parameter Δ will be discussed below. In the cases where the rotational bands were

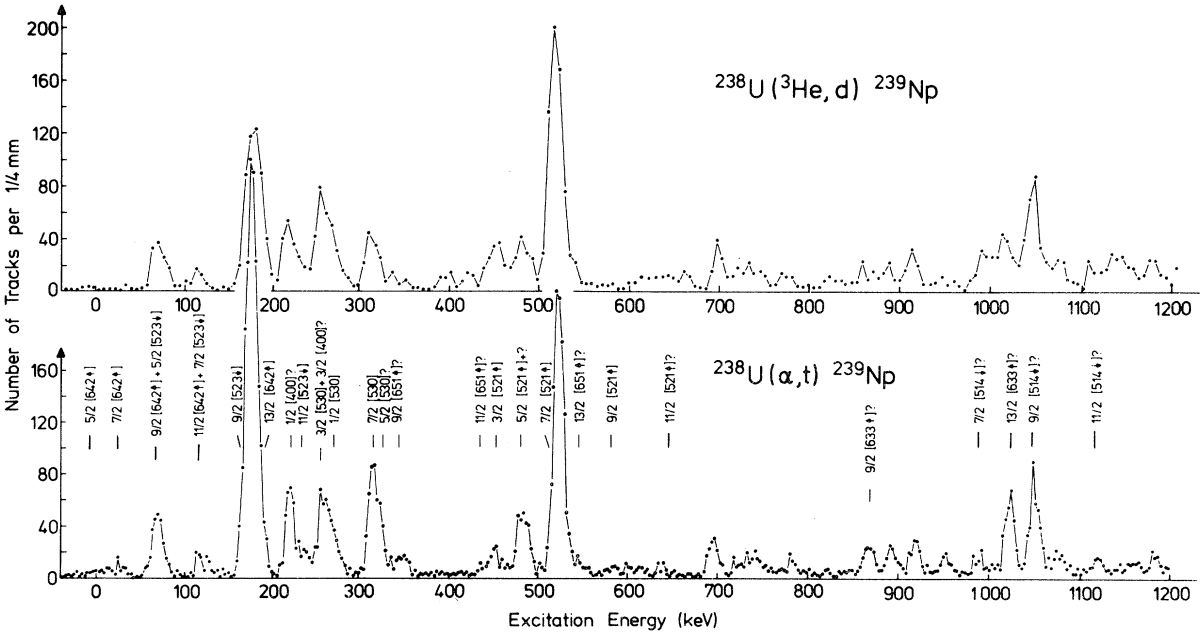

FIG. 1. Measured spectra for the (^{3}He, d) and (α, t) reactions at a laboratory angle of 60°.

TABLE I. Excitation energies and differential cross sections for the (^{3}He, α) and (α,t) reactions.

Energy (keV)	$d\sigma/d\omega$ (^{3}He, d) (μb/sr) 20°	35°	60°	90°	$d\sigma/d\omega$ (α,t) 60° (μb/sr)	$R=\frac{d\sigma(\alpha,t)}{d\sigma(^3\mathrm{He},d)}$ 60°	Probable l value	Suggested assignment
3.3 ± 3.1					0.9 ± 0.3			$\frac{5}{2}^+$[642↑]
27.9 ± 3.1					1.2 ± 0.4			$\frac{7}{2}^+$[642↑]
70.0 ± 1.2		6.7 ± 1.3	3.6 ± 0.4	0.6 ± 0.4	8.9 ± 0.6	2.5 ± 0.3	2, 3, 4	$\frac{9}{2}^+$[642↑] + $\frac{5}{2}^-$[523↓]
117.8 ± 1.6			1.1 ± 0.3		2.3 ± 0.6	2.1 ± 0.8	0–4	$\frac{11}{2}^+$[642↑] + $\frac{7}{2}^-$[523↓]
173.7 ± 1.2	4.1 ± 1.3	8.7 ± 1.7	8.9 ± 1.2	4.4 ± 1.0	27.9 ± 9.0	3.1 ± 1.1	2–6	$\frac{9}{2}^-$[523↓]
180.0 ± 1.2			6.3 ± 1.2		36.4 ± 9.4	5.8 ± 1.9	5, 6	$\frac{13}{2}^+$[642↑]
220.2 ± 1.2	1.9 ± 0.9	5.5 ± 1.1	4.7 ± 0.7		10.8 ± 1.1	2.3 ± 0.5	0–4	$\frac{1}{2}^+$[400]?
239.4 ± 2.1			< 1.0		2.7 ± 0.6	> 2.7	4–6	$\frac{11}{2}^-$[523↓]
258.3 ± 1.3	6.1 ± 1.3	13.3 ± 3.0	5.9 ± 1.0	2.1 ± 0.5	10.6 ± 1.1	1.8 ± 0.4	0–3	$\frac{3}{2}^-$[530] + $\frac{3}{2}^+$[400]?
270.9 ± 1.4			3.2 ± 1.0		4.3 ± 0.8	1.3 ± 0.5	0, 1, 2	$\frac{1}{2}^-$[530]
315.5 ± 1.1	3.6 ± 1.2	6.7 ± 1.3	4.5 ± 0.4	1.7 ± 0.5	14.5 ± 2.0	3.2 ± 0.6	(3)4	$\frac{7}{2}^-$[530]
324.4 ± 4.0					2.4 ± 1.7			$\frac{5}{2}^-$[530]?
346.8 ± 1.4	1.9 ± 0.9	0.7 ± 0.4	0.8 ± 0.4		2.9 ± 0.4	3.6 ± 1.9	2–6	$\frac{9}{2}^+$[651↑]?
420.6 ± 2.2			1.2 ± 0.4		0.3 ± 0.2	0.3 ± 0.2		
436.5 ± 2.7					1.1 ± 0.4			$\frac{11}{2}^+$[651↑]?
449.8 ± 1.1	2.9 ± 1.0	4.9 ± 0.8	3.1 ± 0.4	1.1 ± 0.5	3.2 ± 0.7	1.0 ± 0.3	0, 1	$\frac{3}{2}^-$[521↑]
482.6 ± 1.1		4.7 ± 0.8	3.2 ± 0.4	1.6 ± 0.5	9.9 ± 0.9	3.1 ± 0.5	(3)4, 5	$\frac{5}{2}^-$[521↑]
521.2 ± 1.1	16.3 ± 3.1	24.7 ± 0.8	18.6 ± 0.8	6.6 ± 1.0	40.0 ± 1.2	2.2 ± 0.2	3, 4	$\frac{7}{2}^-$[521↑]
547.0 ± 2.3			< 0.5		1.3 ± 0.4	> 2.6	5, 6	$\frac{13}{2}^+$[651↑]?
581.0 ± 2.2			< 0.5		1.2 ± 0.3	> 2.4	5, 6	$\frac{9}{2}^-$[521↑]
600.4 ± 2.6		1.0 ± 0.4			1.0 ± 0.4			
616.3 ± 2.5			0.9 ± 0.4		0.8 ± 0.4	0.9 ± 0.6	0–3	
637.2 ± 1.8		0.7 ± 0.4	1.1 ± 0.4	2.1 ± 0.6	0.8 ± 0.4	0.7 ± 0.5	0, 1, 2	
657.3 ± 3.1			1.1 ± 0.4					$\frac{11}{2}^-$[521↑]?
695.4 ± 1.1		3.2 ± 0.8	2.7 ± 0.4	1.1 ± 0.5	4.9 ± 0.5	1.8 ± 0.3	3, 4	
723.7 ± 2.2			0.8 ± 0.4	0.8 ± 0.4	1.5 ± 0.6	1.9 ± 1.2		
741.6 ± 2.1		1.9 ± 0.5	1.0 ± 0.4		3.0 ± 1.2	3.0 ± 1.7	2–6	
778.6 ± 1.3		1.7 ± 0.5	1.4 ± 0.4		2.3 ± 0.5	1.6 ± 0.6	0–4	
823.4 ± 1.7		1.8 ± 0.5	1.2 ± 0.4		0.6 ± 0.4	0.5 ± 0.4	0, 1, 2	
864.9 ± 1.2		2.0 ± 0.6	2.1 ± 0.4		4.4 ± 0.5	2.1 ± 0.5	4, 5, 6	$\frac{9}{2}^+$[633↑]?
890.6 ± 1.2		1.2 ± 0.5	1.6 ± 0.4		3.8 ± 0.5	2.4 ± 0.7	4, 5, 6	
917.1 ± 1.1		3.0 ± 0.7	2.6 ± 0.4		4.4 ± 0.5	1.7 ± 0.4	3, 4, 5	
951.5 ± 1.3		1.9 ± 0.6	0.8 ± 0.4	0.9 ± 0.5	2.6 ± 0.4	3.3 ± 1.7	4, 5, 6	
992.9 ± 1.2		3.0 ± 1.6	2.6 ± 0.4	0.9 ± 0.5	2.9 ± 0.5	1.1 ± 0.3	2, 3, 4	$\frac{7}{2}^-$[514↓]?
1019.9 ± 1.2		6.0 ± 2.0	4.5 ± 0.4	2.0 ± 0.6	9.8 ± 0.8	2.2 ± 0.3	5, 6	$\frac{13}{2}^+$[633↑]?
1049.0 ± 1.2		9.1 ± 1.8	8.3 ± 0.6	2.5 ± 0.7	11.9 ± 1.0	1.4 ± 0.2	4(5)	$\frac{9}{2}^-$[514↓]?
1077.2 ± 1.4		2.9 ± 0.8	1.7 ± 0.4		2.8 ± 1.2	1.6 ± 0.8	3–6	

TABLE I. *(Continued)*

Energy (KeV)	$d\sigma/d\omega$ (^{3}He, d) (μb/sr) 20°	35°	60°	90°	$d\sigma/d\omega$ (α,t) 60° (μb/sr)	$R=\frac{d\sigma(\alpha,t)}{d\sigma(^3\mathrm{He},d)}$ 60°	Probable l value	Suggested assignment
1117.8±1.3		3.3±0.8	2.3±0.5		2.5±0.4	1.1±0.3	3, 4, 5	$\frac{11}{2}^-[514\downarrow]$?
1141.1±1.7			2.6±0.5		1.1±0.3	0.4±0.2	0–3	
1155.3±1.9		5.2±0.9	2.1±0.4	1.4±0.5	1.9±0.4	0.9±0.3	2, 3, 4	
1182.5±1.4		3.4±0.8	2.5±0.4		3.5±0.6	1.4±0.4	4, 5, 6	

identified, the experimental single-particle energies defined by $(\epsilon-\lambda)$ were taken, otherwise the theoretical values of this quantity were used (see Table II and discussion below).

D. Normalization factor N

The normalization factor N was determined by comparison of experimental and theoretical cross sections. Although the reaction cross sections may be fragmented by mixing of levels, the sum of the theoretical intensities has to be the same as the sum of the experimental intensities independent of the theoretical assumptions on the mixing. The origin of this sum rule is due to the following relations[19]

$$\sum_{jl} C_{jl,i}{}^2 = 1, \quad \text{and} \quad \sum_{jl} S_{jl,i} = 2U_i{}^2$$

for each Nilsson state. The S_j's may be fragmented by single-particle mixing due to Coriolis interaction, mixing of single-particle states with vibrational states, etc., but the sum over all components in all involved levels has to be $2U_i{}^2$. Since the number of nucleons must be conserved, one finds:

$$2\sum_{i=1}^{n} V_i{}^2 = Z \quad \text{or} \quad 2\sum_{i=1}^{n} U_i{}^2 = (2n-Z),$$

where $Z=92$ for the target nucleus ^{238}U and n is the number of Nilsson states under consideration. The quantity n is taken so large that $U_i{}^2 \approx 1$ for $i>n$. In the present analysis we consider only the 12 Nilsson states from $i=40(\frac{1}{2}^+[660])$ to $i=51(\frac{7}{2}^-[514\downarrow])$. The ground state of ^{239}Np has $i=47(\frac{5}{2}^+[642\uparrow])$. These states have excitation energies below 1200 keV (see Fig. 2) and are not expected to mix strongly with the other states which have excitation energies above 1400 keV. Then

TABLE II. Properties of the rotational bands.

Rotational band	$E_{0\,\mathrm{exp}}$ (keV)	$E_{\mathrm{qp,exp}}$ (keV)	Single-particle energy (keV) $(\epsilon-\lambda)_{\mathrm{exp}}$	$\epsilon_{\mathrm{theor}}$	$(\epsilon-\lambda)_{\mathrm{theor}}$	U^2	Decoupling parameter $a_{1/2\,\mathrm{exp}}$	$a_{1/2\,\mathrm{theor}}$
$\frac{7}{2}^-[514\downarrow]$	(890.6±1.2)	1047	1662	40 840	1640 [a]	0.94		
$\frac{7}{2}^+[633\uparrow]$	(706.6±2.0) [b]	863	1451	40 259	1291 [c]	0.93		
$\frac{3}{2}^-[521\uparrow]$	422.6±0.9 [b]	451	941	40 076	876 [a]	0.86		
$\frac{5}{2}^-[523\downarrow]$	17.7±1.0 [b]	98	332	39 581	381 [a]	0.68		
$\frac{5}{2}^+[642\uparrow]$	−40.7±1.2 [b]	39	72	39 263	295 [c]	0.54		
$\frac{1}{2}^-[530]$	253.0±0.8 [b]	256	−653	38 587	−613 [a]	0.19	−1.38±0.03 [b]	−2.12
$\frac{3}{2}^+[651\uparrow]$	(142.2±2.5) [b]	171	−500	38 463	−505 [c]	0.24		
$\frac{1}{2}^+[400]$	(222.6±1.0)	226	−602	38 307	−661 [c]	0.20	1.08 [d]	0.51
$\frac{3}{2}^-[532\downarrow]$				38 264	−936 [a]	0.13		
$\frac{3}{2}^+[402\downarrow]$				38 095	−873 [c]	0.14		
$\frac{11}{2}^-[505\uparrow]$				38 027	−1173 [a]	0.09		
$\frac{1}{2}^+[660]$				37 991	−977 [c]	0.12		6.62

[a] $\lambda=39\,200$ keV (negative parity).
[b] Obtained from Coriolis calculation.
[c] $\lambda=38\,968$ keV (positive parity).
[d] Value from ^{237}Np.

one obtains:

$$\sum_{i=40}^{51}\sum_{jl} S_{jl,i} = 2\sum_{i=40}^{51} U_i^2 = 10. \qquad (2)$$

If one prefers to sum over cross sections $d\sigma/d\omega$ instead of over S_{jl}'s, one has to make the assumption that the adopted σ_{DWBA} of each pure (not mixed) level is the same as the average σ_{DWBA} of all levels which are mixed with the pure level. This is justified because strong mixing occurs mainly for levels separated by a small energy difference where σ_{DWBA} is nearly constant.

The above sum rule in terms of cross sections can be written in our case:

$$\sum_{i=40}^{51}\sum_{jl} (d\sigma/d\omega)_{i,\,\mathrm{theor}} = \text{total cross section below 1200 keV excitation energy}.$$

The normalization factor N was calculated with this formula to be

$$N(^3\mathrm{He}, d) = 9.4 \quad \text{and} \quad N(\alpha, t) = 160.$$

These values differ by a factor of about 2.2 from literature values[24,2]:

$$N(^3\mathrm{He}, d) = 4.42 \quad \text{and} \quad N(\alpha, t) = 71.$$

E. Pairing gap parameter Δ

The pairing gap parameter Δ was estimated with the simple pairing model from the measured quasiparticle excitation energies E_{qp} and from the measured odd-even mass differences ΔE_{oe}. The experimental E_{qp} values were obtained from the parameters in the rotational formula: $E_I = E_0 + A[I(I+1) + \delta_{K,1/2}(-1)^{I+1/2} a_{1/2}(I+\frac{1}{2})]$ where $E_0 = E_{\mathrm{qp}} - 2AK^2$ ($A = 6.4$ keV, see Sec. VI). The odd-even mass difference was calculated with the masses[18] and the formula[25]:

$$\Delta E_{\mathrm{oe}} = M(^{239}\mathrm{Np}) - [\tfrac{3}{8}M(^{238}\mathrm{U}) + \tfrac{3}{4}M(^{240}\mathrm{Pu}) - \tfrac{1}{8}M(^{242}\mathrm{Cm})]$$

$$= 824 \text{ keV}.$$

The quasiparticle excitation energy is related to the single-particle energy[19] ϵ by

$$E_{\mathrm{qp},i} = [(\epsilon_i - \lambda)^2 + \Delta^2]^{1/2} - [(\epsilon - \lambda)_{\text{ground state}}{}^2 + \Delta^2]^{1/2}$$

and the odd-even mass difference is related to the ground state single-particle energy by[26]

$$\Delta E_{\mathrm{oe}} = [(\epsilon - \lambda)_{\text{ground state}}{}^2 + \Delta^2]^{1/2}.$$

By combining these last two equations one obtains,

$$E_{\mathrm{qp},i} = [(\epsilon_i - \lambda)^2 + \Delta^2]^{1/2} - \Delta E_{\mathrm{oe}}$$

and

$$(\epsilon_i - \lambda)_{\mathrm{exp}} = \pm [(E_{\mathrm{qp},i} + \Delta E_{\mathrm{oe}})^2 - \Delta^2]^{1/2} \qquad (3)$$

and then the combination of the Eqs. (1), (2), and (3) yields:

$$2\sum_{i=40}^{51} U_i^2 = \sum_{i=40}^{51} \left(1 \pm \frac{[(E_{\mathrm{qp},i} + \Delta E_{\mathrm{oe}})^2 - \Delta^2]^{1/2}}{E_{\mathrm{qp},i} + \Delta E_{\mathrm{oe}}}\right) = 10. \qquad (4)$$

The quasiparticle energies of the unidentified bands [532↓], [402↓], [505↑], and [660] were estimated from the Nilsson model. The use of Eq. (4) results in $\Delta = 860$ keV. With this value of Δ and with Eq. (3), the $(\epsilon_i - \lambda)_{\mathrm{exp}}$ values listed in Table II were calculated.

F. Single-particle energies

The Nilsson wave function computer program for the C_{jl}'s[22] also yields single-particle energies $\epsilon_{\mathrm{theor}}$. These values are given in Table II. In order to compare these energies with the experimental values one has to know the Fermi energy λ. This quantity λ is obtained from the experimental energies $(\epsilon_i - \lambda)_{\mathrm{exp}}$ by the relation $\lambda = \epsilon_{\mathrm{theor}} - (\epsilon_i - \lambda)_{\mathrm{exp}}$. The result of this calculation is that λ has two different values, one value for positive parity bands and a slightly different value for negative parity bands. This difference may be caused by special

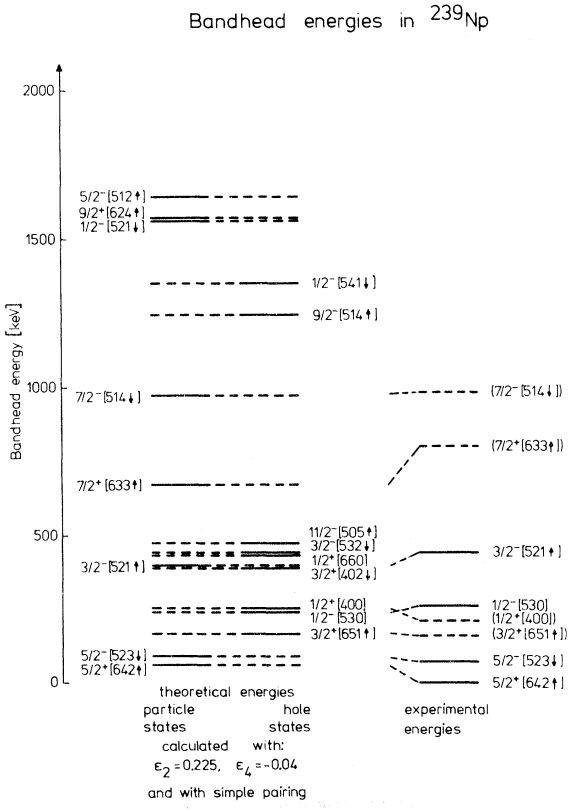

FIG. 2. Theoretical and experimental bandhead energies in ^{239}Np.

features of the theoretical calculations or by special mixing of the bands. In all future calculations we then assume that $\lambda = 38\,968$ keV for positive parity bands and $\lambda = 39\,200$ keV for negative parity bands. With these Fermi energies one obtains the values of $(\epsilon - \lambda)_{\text{theor}}$ as given in Table II and the theoretical bandhead energies shown in Fig. 2. It has to be pointed out that all these pairing calculations are only approximate. For example, Δ may have different values for different configurations.

IV. LEVEL SCHEME OF ^{239}Np FROM γ RAYS FOLLOWING THE DECAY OF ^{239}U

Cline and Tripp[8] recently measured γ rays in ^{239}Np from the decay of ^{239}U. These authors added a note to their level scheme in *Nuclear Data Sheets* indicating that all levels above 0.4 MeV should be considered as tentative. Based on their data[8] we constructed a level scheme which is consistent with α-decay measurements, energy combinations, and the present reaction results. This level scheme is shown in Fig. 3. The level energies and errors were obtained from a least squares fit to the transition energies. Most of the stronger γ-ray transitions are included in this level scheme. The levels at 220.52 and 333.13 keV are not well established. All levels in our level scheme seem to correspond to levels observed in the (^{3}He, d) and (α, t) reaction except the levels at 518.00, 662.24, 844.98, and 964.23 keV which may be vibrational excitations. Only the levels at 220.52, 333.13, 824.83, and 865.92 keV in our level scheme are not shown in the level scheme of Cline and Tripp.[8] The 662.24-keV level in our level scheme is probably the same as the 666-keV level of Lederer *et al.*[14] and might be identified as a vibrational state.

V. ROTATIONAL BANDS

The identified rotational bands and the levels excited by the (^{3}He, d) and (α, t) reactions are shown on the left side of Fig. 3. Experimental and theoretical energies and experimental and theoretical cross sections of the individual levels of the rotational bands are given in Table III.

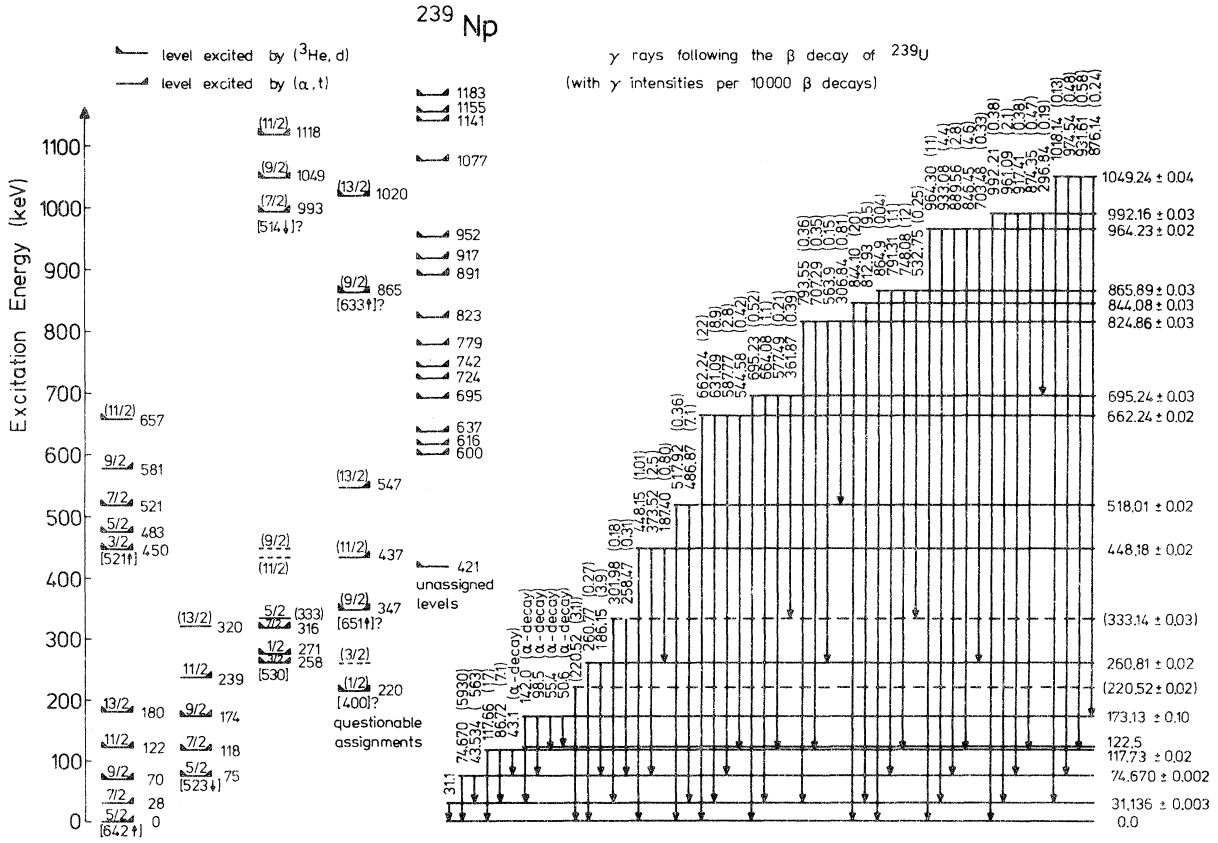

FIG. 3. Level scheme of ^{239}Np.

TABLE III. Experimental and theoretical energies and cross sections of the rotational bands.

Rotational band	Level	$E_{\alpha,\beta,\gamma}$ (keV)	E_{react} (keV)	E_{calc} (keV)	$d\sigma/d\omega$ (^{3}He, d) (μb/sr) 60° Exp.	Theoretical Without Coriolis	Theoretical With Coriolis	$N\sigma_{\text{DWBA}}$	$d\sigma/d\omega$ (α, t) (μb/sr) 60° Exp.	Theoretical Without Coriolis	Theoretical With Coriolis	$N\sigma_{\text{DWBA}}$
$\frac{7}{2}^-[514\downarrow]$	$\frac{7}{2}$	(992.16 ±0.03)	(992.9 ± 1.2)	991.4 [a]	(2.6 ± 0.4)	0.60		25.8	(2.9 ± 0.5)	0.72		31.3
	$\frac{9}{2}$	(1049.2 ±0.04)	(1049.0 ± 1.2)	1049.0	(8.3 ± 0.6)	11.8		6.4	(11.9 ± 1.0)	23.92		14.1
	$\frac{11}{2}$		(1117.8 ± 1.3)	1119.4	(2.3 ± 0.5)	0.13		6.6	(2.5 ± 0.4)	0.24		13.7
$\frac{7}{2}^+[633\uparrow]$	$\frac{7}{2}$			807.5 [b]		0.010	0.009	21.2		0.019	0.018	41.4
	$\frac{9}{2}$	(865.89 ±0.03)	(864.9 ± 1.2)	865.3	(2.1 ± 0.4)	0.72	0.69	21.6	(4.4 ± 0.5)	1.34	1.28	40.1
	$\frac{11}{2}$			935.9		0.072	0.069	4.8		0.23	0.22	14.8
	$\frac{13}{2}$			1019.4	(4.5 ± 0.4)	8.88	8.50	4.9	(9.8 ± 0.8)	26.30	25.18	14.6
$\frac{3}{2}^-[521\uparrow]$	$\frac{3}{2}$	448.18 ±0.02	449.8 ± 1.1	446.7 [b]	3.1 ± 0.4	3.15	3.00	33.9	3.2 ± 0.7	4.38	4.17	47.1
	$\frac{5}{2}$		(482.6 ± 1.1)	479.6	(3.2 ± 0.4)	0.54	0.57	22.2	(9.9 ± 0.9)	1.09	1.15	44.8
	$\frac{7}{2}$		521.2 ± 1.1	525.2	18.6 ± 0.8	29.44	28.59	22.6	40.0 ± 1.2	56.99	55.34	43.7
	$\frac{9}{2}$		581.0 ± 2.2	584.6		1.01	0.54	5.9	1.2 ± 0.3	2.96	1.58	17.2
	$\frac{11}{2}$		(657.3 ± 3.1)	655.8	1.1 ± 0.4	0.62	0.61	6.0		1.72	1.70	16.8
$\frac{5}{2}^-[523\downarrow]$	$\frac{5}{2}$	74.67 ±0.002	70.0 ± 1.2 [c]	73.2 [b]	3.6 ± 0.4 [c]	0.56	0.52	19.3	8.9 ± 0.6 [c]	1.61	1.51	55.5
	$\frac{7}{2}$	117.73 ±0.02	117.8 ± 1.6 [c]	117.3	1.1 ± 0.3 [c]	0.77	0.36	19.5	2.3 ± 0.6 [c]	2.14	0.99	54.2
	$\frac{9}{2}$	173.13 ±0.10	173.7 ± 1.2	174.0	8.9 ± 1.2	6.71	7.04	5.3	27.9 ± 9.0	25.45	26.72	20.2
	$\frac{11}{2}$	241 ±1.0	239.4 ± 2.1	243.4		0.16	0.11	5.3	2.7 ± 0.6	0.58	0.39	19.7
$\frac{5}{2}^+[642\uparrow]$	$\frac{5}{2}$	0.0	3.3 ± 3.1	1.8 [b]		0.12	0.21	34.8	0.9 ± 0.3	0.33	0.56	94.1
	$\frac{7}{2}$	31.136 ± 0.003	27.9 ± 3.1	30.1		0.025	0.038	17.4	1.2 ± 0.4	0.087	0.13	60.5
	$\frac{9}{2}$		70.0 ± 1.2 [c]	69.3	3.6 ± 0.4 [c]	0.84	1.40	17.4	8.9 ± 0.6 [c]	2.91	4.86	60.3
	$\frac{11}{2}$	122.5	117.8 ± 1.6 [c]	120.1	1.1 ± 0.3 [c]	0.039	0.054	4.2	2.3 ± 0.6 [c]	0.15	0.20	15.9
	$\frac{13}{2}$		180.0 ± 1.2	182.8	6.3 ± 1.2	4.42	6.63	4.3	36.4 ± 9.4	16.44	24.62	16.2
$\frac{1}{2}^-[530]$	$\frac{1}{2}$		270.9 ± 1.4	266.7 [b]	3.2 ± 1.0	0.25	0.25	31.0	4.3 ± 0.8	0.45	0.45	54.2
	$\frac{3}{2}$	260.81 ±0.02	258.3 ± 1.3 [c]	259.2	5.9 ± 1.0 [c]	2.20	2.34	31.0	10.6 ± 1.1 [c]	3.85	4.09	54.2
	$\frac{5}{2}$	333.14 ±0.03	(324.4 ± 4.0)	335.1		0.006	0.014	21.2	(2.4 ± 1.7)	0.013	0.033	48.7
	$\frac{7}{2}$		315.5 ± 1.1	317.9	4.5 ± 0.4	4.03	5.28	21.0	14.5 ± 2.0	9.34	12.2	48.7

TABLE III *(Continued)*

Rotational band	Level	$E_{\alpha,\beta,\gamma}$ (keV)	E_{react} (keV)	E_{calc} (keV)	$d\sigma/d\omega$ (^{3}He,d) (μb/sr) 60° Exp.	Theoretical Without Coriolis	Theoretical With Coriolis	$N\sigma_{DWBA}$	$d\sigma/d\omega$ (α,t) (μb/sr) 60° Exp.	Theoretical Without Coriolis	Theoretical With Coriolis	$N\sigma_{DWBA}$
$\frac{1}{2}^-[530]$	$\frac{9}{2}$			454.0		0.39	0.49	5.7		1.26	1.57	18.4
	$\frac{11}{2}$			427.5		0.22	0.28	5.7		0.70	0.90	18.4
$\frac{3}{2}^+[651\uparrow]$	$\frac{3}{2}$			166.2 [b]		0.041	0.041	37.9		0.091	0.091	84.7
	$\frac{5}{2}$			211.6		0.24	0.14	38.6		0.51	0.31	82.5
	$\frac{7}{2}$			272.8		0.017	0.004	18.5		0.050	0.012	54.2
	$\frac{9}{2}$		(346.8 ± 1.4)	348.6	(0.8 ± 0.4)	0.72	0.13	18.9	(2.9 ± 0.4)	2.01	0.37	52.9
	$\frac{11}{2}$		(436.5 ± 2.7)	438.4		0.013	0.000	4.5	(1.1 ± 0.4)	0.041	0.000	14.8
	$\frac{13}{2}$		(547.0 ± 2.3)	541.8		1.94	0.007	4.5	(1.3 ± 0.4)	6.19	0.022	14.4
$\frac{1}{2}^+[400]$	$\frac{1}{2}$	(220.52 ± 0.02)	(220.2 ± 1.2)	220.5 [a]	(4.7 ± 0.7)	13.58		48.1	(10.8 ± 1.1)	23.06		81.6
	$\frac{3}{2}$		(258.3 ± 1.3) [c]	260.4	(5.9 ± 1.0) [c]	3.18		39.1	(10.6 ± 1.1) [c]	6.60		81.2
	$\frac{5}{2}$		(258.3 ± 1.3) [c]	257.9	(5.9 ± 1.0) [c]	1.11		39.1	(10.6 ± 1.1) [c]	2.30		81.2
	$\frac{7}{2}$			351.1		0.088		18.9		0.24		52.4
	$\frac{9}{2}$			346.5		0.032		18.9		0.89		52.4
$\frac{3}{2}^-[532\downarrow]$	$\frac{3}{2}$			442 [d]		0.069		33.7		0.094		45.7
	$\frac{5}{2}$			474		0.50		22.2		1.02		44.8
	$\frac{7}{2}$			519		0.26		22.6		0.50		43.6
	$\frac{9}{2}$			576		1.26		5.9		3.73		17.4
	$\frac{11}{2}$			647		0.053		6.0		0.15		16.9
$\frac{3}{2}^+[402\downarrow]$	$\frac{3}{2}$			396 [d]		10.74		41.6		19.05		73.8
	$\frac{5}{2}$			428		0.48		42.0		0.82		72.1
	$\frac{7}{2}$			473		0.022		19.6		0.42		49.4
	$\frac{9}{2}$			530		0.003		19.9		0.008		48.0
$\frac{11}{2}^-[505\uparrow]$	$\frac{11}{2}$			472 [d]		1.03		5.7		3.24		18.0

TABLE III (*Continued*)

Rotational band	Level	$E_{\alpha,\beta,\gamma}$ (keV)	E_{react} (keV)	E_{calc} (keV)	$d\sigma/d\omega$ (^{3}He, d) (μb/sr) 60° Exp.	Theoretical Without Coriolis	Theoretical With Coriolis	$N\sigma_{\text{DWBA}}$	$d\sigma/d\omega$ (α, t) (μb/sr) 60° Exp.	Theoretical Without Coriolis	Theoretical With Coriolis	$N\sigma_{\text{DWBA}}$
$\frac{1}{2}^+$[660]	$\frac{1}{2}$			437 [d]		0.099		52.8		0.13		68.1
	$\frac{3}{2}$			584		0.044		44.7		0.063		64.1
	$\frac{5}{2}$			404		0.17		41.6		0.30		73.3
	$\frac{7}{2}$			745		0.006		21.0		0.012		42.8
	$\frac{9}{2}$			422		0.48		19.3		1.26		50.6
	$\frac{11}{2}$			958		0.002		4.9		0.004		11.8
	$\frac{13}{2}$			490		0.93		4.5		2.83		13.7

[a] Extrapolated with rotational formula and $A = 6.4$ keV.
[b] Fitted with Coriolis interaction.
[c] Several lines contribute to this value.
[d] Calculated from single-particle energies of the Nilsson model and $A = 6.4$ keV.

A. $\frac{5}{2}^+$[642↑] ground state band

The ground state band is well established.[27] All levels up to $\frac{13}{2}$ are observed in the (α, t) reaction. This band has a very narrow spacing ($A = 4.4$ keV) and one expects strong Coriolis mixing with the $\frac{3}{2}^+$[651↑] band. The other candidate for strong Coriolis coupling, the $\frac{7}{2}^+$[633↑] band, is predicted to be at a higher excitation energy (see Fig. 2). A difficulty in the determination of the reaction cross sections of the levels in this band is the fact that the $\frac{9}{2}$, $\frac{11}{2}$, and $\frac{13}{2}$ levels are very close to the $\frac{5}{2}$, $\frac{7}{2}$, and $\frac{9}{2}$ levels, respectively, of the [523↓] band. Taking this into consideration, the cross sections are in reasonable agreement with the theory.

B. $\frac{5}{2}^-$[523↓]

This band is favored in the α decay from ^{243}Am. The four lowest levels of this band are seen in the (α, t) reaction, but three of them are not resolved from levels of the [642↑] band. The cross section of the $\frac{11}{2}$ member is larger than expected from theory. The other cross sections are in good agreement with the theoretical values. The rotational parameter of $A = 6.1$ keV for this band indicates weak Coriolis mixing.

C. $\frac{1}{2}^-$[530]

This configuration is the ground state in the Pa isotopes.[1] Baranov, Kulakov, and Shatinsky[13] and Lederer *et al.*[14] interpreted the 267-keV level to be the $\frac{3}{2}$ member of this band by analogy with ^{237}Np. The decoupling parameter predicts that the $\frac{1}{2}$ and $\frac{3}{2}$ levels (~260 keV) are close in energy as are the $\frac{5}{2}$ and $\frac{7}{2}$ levels (~320 keV). According to our level scheme the $\frac{3}{2}$ and $\frac{5}{2}$ levels of the $\frac{1}{2}^+$[400] band are expected also around 260 keV. Therefore, only unresolved groups are seen in the reaction spectra and in the α-decay spectra. From the γ decay of the 260.81-keV level and the 333.13-keV level, we conclude that these levels are the $\frac{3}{2}$ and $\frac{5}{2}$ members of the [530] band. The $\frac{7}{2}$ member is predicted to have the largest reaction cross section. Both the reaction cross section and the l value of the 315.5-keV level are in agreement with the $\frac{7}{2}^-$[530] assignment. The experimental cross section of the 258.3-keV level is in agreement with the sum of the theoretical cross sections for the $\frac{3}{2}^-$[530], $\frac{3}{2}^+$[400], and $\frac{5}{2}^+$[400] levels. In view of these arguments we consider this band as well established. The rotational parameter $A = 5.97$ keV and the decoupling parameter $a_{1/2} = -1.42$ (calculated without correcting for Coriolis coupling).

D. $\frac{3}{2}^-$[521↑]

The level in ^{239}Np which has the largest theoretical cross section is the $\frac{7}{2}$ member of the [521↑]

TABLE IV. Coriolis interaction parameters.

Rotational bands	$A_{K\,\mathrm{exp}}$	$A_{K\,\mathrm{theor}}$	$\langle K\|j-\|K+1\rangle_{\mathrm{theor}}$
[660] −[402↓]		−1.9	0.29
[660] −[651↑]		−41.8	6.62
[400] −[402↓]		−4.5	0.70
[400] −[651↑]		−3.4	0.53
[402↓] −[642↑]		−2.4	0.41
[651↑] −[642↑]	−23.0 ± 0.3	−39.5	6.50
[642↓] −[633↑]	−3.8 ± 5.7	−35.3	6.21
[530] −[532↓]		−5.5	0.86
[530] −[521↑]	−2.9 ± 2.2	−17.5	3.76
[532↓] −[523↓]		−23.2	4.39
[521↑] −[523↓]	−6.3 ± 1.9	−3.9	0.61
[523↓] −[514↓]		−23.7	3.94

band. The largest experimental cross section populates the level at 521.2 keV. The experimental l value and the theoretical bandhead energy (Fig. 2) support a $\frac{7}{2}^-$[521↑] assignment for the 521.2-keV level. The level at 448.18 keV was observed with the reaction cross section and γ-ray branching ratios expected for the bandhead $\frac{3}{2}^-$[521↑]. The 482.6-keV level (Table I) may be a doublet and is tentatively assigned as the $\frac{5}{2}$ member. The $\frac{9}{2}$ and the $\frac{11}{2}$ members are also seen in the reaction spectrum. The rotational parameter A calculated with the energies of the $\frac{3}{2}$ and $\frac{7}{2}$ levels is 6.09 keV. The [521↑] band is the ground state band of the ^{243}Bk, ^{245}Bk, and ^{247}Bk isotopes.[1] The experimental cross section of the $\frac{7}{2}$ member is smaller than the theoretical value and may be the result of mixing with vibrational states.[28] The 695-keV level has a similar experimental l value as the $\frac{7}{2}$ [521↑] level. It may be a $\frac{7}{2}$ member of a vibrational state mixed with the [521↑] band.

E. $\frac{1}{2}^+$[400]

In ^{237}Np the [400] bandhead was observed at 332 keV. The theoretical bandhead energy (Fig. 2) of this level is just above the $\frac{1}{2}^-$[530] level. The 220.2-keV level is a likely choice for this bandhead. The observed reaction cross section is somewhat smaller than the theoretical value. This level is also seen in the α spectrum[13,15] of ^{243}Am, but was considered an impurity. The α intensity of this line is the same as that of the $\frac{1}{2}^+$[400] level in ^{237}Np.[14] By comparison[17] with ^{237}Np, the $\frac{3}{2}$ and $\frac{5}{2}$ members are at 39 and 36 keV, respectively, above the bandhead. The level group at 258.3 keV has the theoretically expected cross section (see $\frac{3}{2}^-$[530]). The 220.2-keV $\frac{1}{2}^+$[400] level can decay only to the ground state. Hence, the 220.52-keV transition is tentatively placed between the 220.2-keV level and the ground state because there is no other γ line with the appropriate energy. The identification of the [400] band is probable.

F. $\frac{3}{2}^+$[651↑]

As pointed out in the discussion of the [642↑] band, this band is expected to mix by Coriolis coupling with the [651↑] band. The Coriolis matrix element is rather large (Table IV). The theoretical bandhead energy of the [651↑] band is near 170 keV. In order to identify the $\frac{13}{2}$ member of this band, we looked for a $l=6$ transition to a level of energy around 500 keV. Candidates for the $\frac{9}{2}$, $\frac{11}{2}$, and $\frac{13}{2}$ states of this band are the observed levels at 346.8, 436.5, and 547.0 keV. Although these levels are in agreement with both the energies and the matrix element of the Coriolis calculation (Sec. VI), this assignment is very tentative.

G. $\frac{7}{2}^+$[633↑] and $\frac{7}{2}^-$[514↓]

There are two strong lines in the reaction spectra above 1.0 MeV with $l=5$ or 6 and $l=4$ or 5, respectively. On the basis of the theoretical energies and cross sections one might identify the 1019.9-keV level as the $\frac{13}{2}^+$[633↑] state and the 1049.0-keV level as the $\frac{9}{2}^-$[514↓] state. The 992.9-(992.18-) and 1117.8-keV levels are possibly the $\frac{7}{2}$ and $\frac{11}{2}$ members of the [514↓] band. If the 864.9-keV level is the $\frac{9}{2}$ member of the [633↑] band, it is not identical with the 865.92-keV level in the γ-decay scheme. Fragmentation of the single-particle strength by mixing with vibrational states may explain why the reaction cross sections of the $\frac{13}{2}^+$[633↑] and $\frac{9}{2}^-$[514↓] levels are smaller than predicted by theory. At present we see no alternatives to these identifications, and we consider them both as probable.

VI. DISCUSSION

A. Coriolis interaction

With the coefficients of the wave functions C_{jl} and the pairing emptiness U^2, one can calculate theoretical Coriolis matrix elements $\langle K|\,j-|\,K+1\rangle$ and theoretical Coriolis interaction parameters[19] A_K. These values listed in Table IV show which bands are likely to mix strongly by Coriolis interaction. Experimental Coriolis interaction parameters were obtained with a computer program[29] by fitting the level energies calculated with the interaction parameters A_K, the band energies E_0, and the decoupling parameter $a_{1/2}$ to the experimental level energies. Calculations were performed for three positive parity bands, [642↑], [651↑], and [633↑] and for three negative parity bands, [523↓], [530], and [521↑]. The rotational parameter A was assumed to be 6.4 keV for all bands. Since additional rotational bands may contribute to the Coriolis mixing and $\Delta N=2$ mixing was neglected, these three band mixing calculations are only ap-

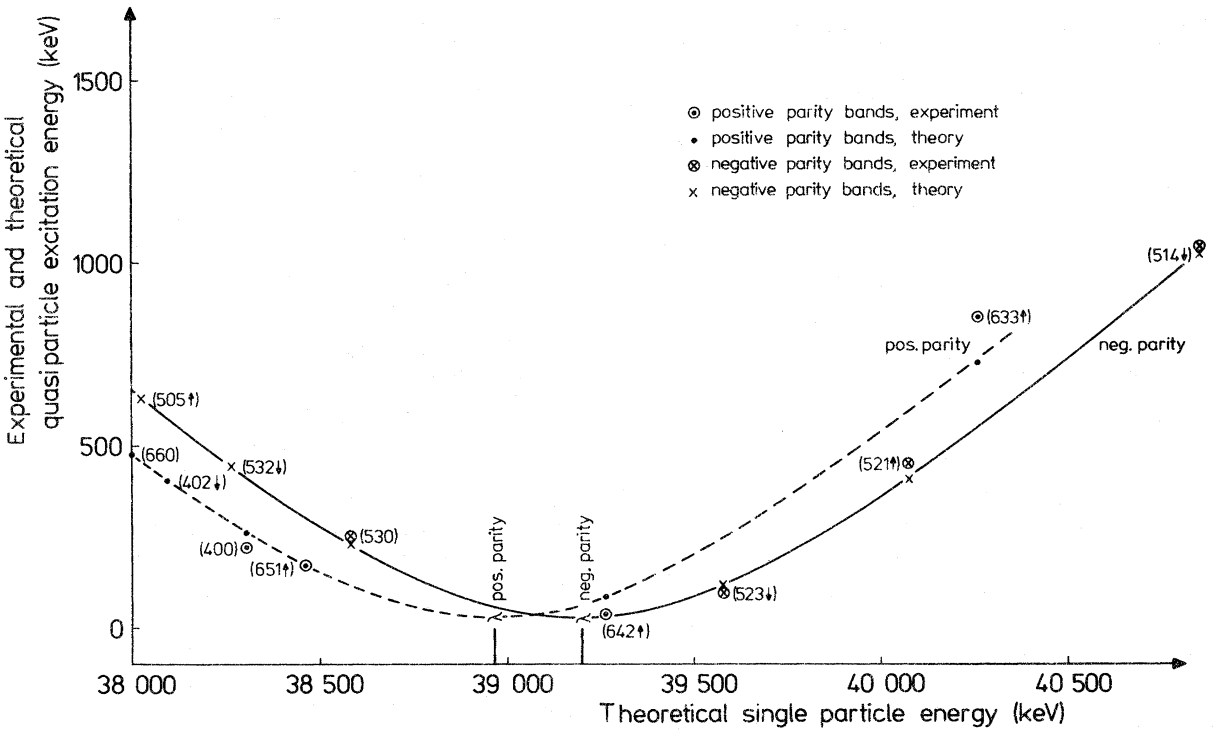

FIG. 4. Experimental quasiparticle excitation energy as a function of the theoretical single-particle energy.

proximate.

The fitted values of $A_{K\,\mathrm{exp}}$ are given in Table IV. They have the same sign and are smaller than the theoretical values in most cases. Because of the above mentioned uncertainties, a more detailed comparison is not meaningful.

The fitted E_0 energies and the decoupling parameter a are listed in Table II (marked with b). The fitted level energies are given in Table III as E_{calc} (marked with b). The agreement between fitted and measured level energies is good and indicates that the level identification is consistent.

The Coriolis calculation also yields cross sections for the (^{3}He, d) and (α, t) reactions (see Table III). There are only a few cases where one observes a significant change in the cross section by the Coriolis mixing. These changes are, in most cases, of the same order of magnitude as the experimental error.

B. Single-particle energies

Experimental energies $(\epsilon - \lambda)_{\mathrm{exp}}$ have been calculated as described in Sec. III. These energies are listed in Table II and agree very well with the theoretical energies $(\epsilon - \lambda)_{\mathrm{theor}}$. The average difference between experimental and theoretical quasiparticle energies E_{qp} is 41 keV. This good agreement is shown in Fig. 2 for the bandhead energies. In Fig. 4 is shown the experimental quasiparticle excitation energies $E_{\mathrm{qp,\,exp}}$ as a function of the theoretical single-particle energies. The curves represent the theoretical quasiparticle excitation energies calculated from the single-particle energies. One sees that bands with different parity correspond to different Fermi energies λ.

C. Unidentified rotational bands

Figure 2 demonstrates that in ^{239}Np there is a very large density of rotational bands below 1 MeV. This makes the identification of all bands very difficult. Four expected bands were not found: $\frac{3}{2}^+[402\downarrow]$, $\frac{1}{2}^+[660]$, $\frac{3}{2}^-[532\downarrow]$, and $\frac{11}{2}^-[505\uparrow]$. They have smaller theoretical cross sections because they are hole states. From these bands, the $\frac{3}{2}^+[402\downarrow]$ level is expected to have the largest cross section. There is no good candidate for this line with the predicted cross section and the predicted l value. The fact that this line was not observed may be due to its being obscured by another line, its intensity shifted by Coriolis mixing to the [400] band, or its U^2 being smaller than calculated. Most of the other levels have cross sections which are too small to be observed (see Table III).

*Work supported by the U.S. Atomic Energy Commission.
†Supported by a grant from the National Science Foundation.

[1]Y. A. Ellis and M. R. Schmorak, Nucl. Data B8, 345 (1972).
[2]Th. W. Elze and J. R. Huizenga, Phys. Rev. C 1, 328 (1970).
[3]Th. W. Elze and J. R. Huizenga, Nucl. Phys. A149, 585 (1970).
[4]J. R. Huizenga, L. B. Magnusson, M. S. Freedman, and F. Wagner, Jr., Phys. Rev. 84, 1264 (1951).
[5]K. J. Blinowska, P. G. Hansen, H. L. Nielsen, O. Schult, and K. Wien, Nucl. Phys. 55, 331 (1964).
[6]B. P. K. Maier, Z. Phys. 184, 143 (1965).
[7] D. R. Mackenzie and R. D. Connor, Nucl. Phys. A108, 81 (1968).
[8]J. E. Cline and D. A. Tripp, private communication cited in Nucl. Data B6, 577 (1971).
[9]F. Asaro and I. Perlman, Phys. Rev. 93, 1423 (1954).
[10]F. Stephens, J. Hummel, F. Asaro, and I. Perlman, Phys. Rev. 98, 261 (1955).
[11]F. Asaro, F. S. Stephens, J. M. Hollander, and I. Perlman, Phys. Rev. 117, 492 (1960).
[12]P. R. Christensen, Nucl. Phys. 41, 17 (1963).
[13]S. A. Baranov, V. M. Kulakov, and V. M. Shatinsky, Nucl. Phys. 56, 252 (1964).
[14]C. M. Lederer, J. K. Poggenburg, F. Asaro, J. O. Rasmussen, and I. Perlman, Nucl. Phys. 84, 481 (1966).
[15]J. R. Van Hise and D. Engelkemeir, Phys. Rev. 171, 1325 (1968).
[16]D. Engelkemeir, Phys. Rev. 181, 1675 (1969).
[17]Y. A. Ellis, Nucl. Data B6, 539 (1971).
[18]A. H. Wapstra and N. B. Gove, Nucl. Data A9, 265 (1971).
[19]B. Elbek and P. O. Tjøm, in *Advances in Nuclear Physics*, edited by M. Baranger and E. Vogt (Plenum, New York, 1969), Vol. 3, p. 259.
[20]B. H. Wildenthal, B. M. Preedom, E. Newmann, and M. R. Cates, Phys. Rev. Lett. 19, 960 (1967).
[21]J. S. Lilley and N. Stein, Phys. Rev. Lett. 19, 709, 1000 (1967).
[22]B. Nilsson, Nucl. Phys. A129, 445 (1969).
[23]S. G. Nilsson, C. F. Tsang, A. Sobiczewski, Z. Szymanski, S. Wycech, C. Gustafson, I.-L. Lamm, P. Möller, and B. Nilsson, Nucl. Phys. A131, 1 (1969).
[24]R. H. Bassel, Phys. Rev. 149, 791 (1966).
[25]H. J. Mang, J. K. Poggenburg, and J. O. Rasmussen, Nucl. Phys. 64, 353 (1965).
[26]J. M. Eisenberg and W. Greiner, *Microscopic Theory of the Nucleus* (North-Holland, Amsterdam-London, 1972), p. 334.
[27]A. Artna-Cohen, Nucl. Data B6, 577 (1971).
[28]F. A. Gareev, S. P. Ivanova, L. A. Malov, and V. G. Soloviev, Nucl. Phys. A171, 134 (1971).
[29]Program by W. Henning, Technical University Munich, private communication.